

Fungal loop transfer of N depends on biocrust constituents and N form

2

Zachary T. Aanderud¹, Trevor B. Smart¹, Nan Wu², Alexander S. Taylor¹,

4 **Yuanming Zhang², Jayne Belnap³**

6 ¹Department of Plant and Wildlife Sciences, Brigham Young University, Provo, Utah
84602, USA

8 ²Xinjiang Institute of Ecology and Geography, Key Laboratory of Biogeography and
Bioresource in Arid Land, Chinese Academy of Sciences, Urumqi 830011, China

10 ³US Geological Survey, Southwest Biological Science Center, 2290 S. Resource
Blvd., Moab, UT 84532, USA

12

Running head: dark septate fungi translocate ammonium in biocrusts

14

Key words: ammonium, Ascomycota, Colorado Plateau, dark septate endophyte,

16 fungal loop, Indian ricegrass, Pleosporales

Correspondence to: Zachary T. Aanderud (zachary_aanderud@byu.edu)

18

20 **Abstract.** Besides performing multiple ecosystem services individually and
collectively, biocrust constituents may also create biological networks connecting
22 spatially and temporally distinct processes. In the fungal loop hypothesis, rainfall
variability allows fungi to act as conduits and reservoirs, translocating resources
24 between soils and host plants. To evaluate the extent biocrust species composition and
N form influence loops, we created a minor, localized rainfall event containing
26 $^{15}\text{NH}_4^+$ and $^{15}\text{NO}_3^-$ and measured the resulting $\delta^{15}\text{N}$ in the surrounding dry
cyanobacteria- and lichen-dominated crusts and grass, *Achnatherum hymenoides*,
28 after twenty-four hours. We also estimated the biomass of fungal constituents using
quantitative PCR and characterized fungal communities by sequencing the 18S rRNA
30 gene. We found evidence for the initiation of fungal loops in cyanobacteria-
dominated crusts where ^{15}N , from $^{15}\text{NH}_4^+$, moved 40 mm h^{-1} in biocrust soils with the
32 $\delta^{15}\text{N}$ of crusts decreasing as the radial distance from the water addition increased
(linear mixed effects model (LMEM): $R^2 = 0.67$, $F_{2,12} = 11$, $P = 0.002$). In
34 cyanobacteria crusts, $\delta^{15}\text{N}$, from $^{15}\text{NH}_4^+$, was diluted as Ascomycota biomass
increased (LMEM: $R^2 = 0.63$, $F_{2,8} = 6.8$, $P = 0.02$), Ascomycota accounted for 82%
36 (± 2.8) of all fungal sequences, and one order, Pleosporales, comprised 66% (± 6.9) of
Ascomycota. The seeming lack of loops in moss-dominated crusts may stem from the
38 relatively large moss biomass effectively absorbing and holding N from our minor
wet deposition event. The substantial movement of $^{15}\text{NH}_4^+$ may indicate a fungal
40 preference for the reduced N form during amino acid transformation and
translocation. We found a marginally significant enrichment of $\delta^{15}\text{N}$ in *A. hymenoides*

42 leaves but only in cyanobacteria biocrusts translocating ^{15}N , offering evidence of
links between biocrust constituents and higher plants. Our results suggest that minor
44 rainfall events may initiate fungal loops potentially allowing constituents, like dark
septate Pleosporales, to rapidly translocate N from NH_4^+ over NO_3^- through biocrust
46 networks.

48 **1 Introduction**

Fungi may act as conduits for biological networks connecting belowground
ecosystem processes to plants. Soil fungi contribute to all aspects of litter
decomposition through the generation of a myriad of extracellular enzymes (Osono
2007, Schneider et al. 2012); altered trophic dynamics, decomposer species diversity,
and nutrient turnover rates (Hattenschwiler et al. 2005); and by forming multiple
types of endophyte-plant symbioses (Johnson et al. 1997, Saikkonen et al. 2004).
Endophytic fungi, in particular, form hubs connecting spatially and temporally
distinct microbial-mediated soil processes and plants. For example, the pervasive
distribution of mycorrhizae in mesic systems allows common mycorrhizal networks
to deliver essential resources, which promotes or hinders seedling growth depending
on the network species composition (van der Heijden and Horton 2009), and
facilitates the one-way transfer of multiple forms of N and P between two plant
species linked by arbuscular mycorrhizae and ectomycorrhizae (He et al. 2003,
Walder et al. 2012). In xeric systems, endophytic fungi are also implicated in moving
resources within biological networks in a theory known as the fungal loop hypothesis.
The hypothesis states that fungi, supported by biotrophic C from plants and terrestrial
cyanobacteria, act as intermediate reservoirs transforming and translocating resources
between soils and plants (Collins et al. 2008, 2014). Perhaps the most notable
example of a fungal loop, albeit from a limited number of studies, occurred in fungal-
dominated cyanobacteria biocrusts from a Chihuahuan Desert grassland. Specifically,
 $^{15}\text{NO}_3^-$ applied to a root-free biocrust rapidly moved into the perennial grass,

70 *Bouteloua* sp., up to 1 m away within 24–hours (Green et al. 2008). Furthermore, ¹³C-
labeled glutamic acid applied to leaf surfaces of *Bouteloua* was found in biocrusts.

72 Despite the intriguing evidence, many aspects of this burgeoning hypothesis remain to
be validated (Collins et al. 2014).

74

Biocrust composition and soil moisture availability interactions may dictate the
76 movement of resources in fungal loops. Desert fungal-plant interactions occur across
spatially discontinuous patches of vegetation interspersed by patches of soils
78 colonized by biocrusts (Belnap et al. 2005). Fungi participating in loops are
necessarily associated with a mosaic of other biocrust organisms (i.e., cyanobacteria,
80 green algae, lichens, mosses, and other bacteria). The metabolic activity of biocrust
constituents participating in fungal loops, including plants, are moisture-dependent
82 and regulated by the magnitude and seasonality of episodic rainfall events. A pulse-
reserve paradigm (Collins et al. 2008) may explain biological activities where minor
84 rainfall pulses stimulate microorganisms, generating reserves of resources to be
exploited during subsequent rainfall events (Huxman et al. 2004, Welter et al. 2005).

86 In such loops, minor rainfall events may stimulate N₂ fixation by free or lichen-
associated cyanobacteria (Belnap et al. 2003), N mineralization by bacteria and fungi
88 (Cable and Huxman 2004, Yahdjian and Sala 2010), and nitrification and possibly
denitrification (Wang et al. 2014), potentially altering levels of NH₄⁺ or NO₃⁻. Fungal
90 species, including fungal endophytes, may compete with mosses, lichen,
cyanobacteria, and other bacteria for newly released N. Once sequestered, the N may

92 be transformed into amino acids and transported within mycelium (Jin et al. 2012,
Behie and Bidochka 2014). Larger rainfall events may then activate plants, allowing
94 the host plant to receive N from the fungi and transfer photosynthate to the fungal
endophyte. If fungal endophytes are poor competitors for newly released N,
96 preferentially sequester one inorganic N form over another, or more efficiently
transform and transport NH_4^+ rather than NO_3^- , biocrust constituents and N form may
98 influence the translocation of N in fungal loops.

100 The fungal endophytes most likely involved in the loop hypothesis are dark septate
fungi. Few arbuscular mycorrhizal fungi are found in biocrusts (Porrás-Alfaro et al.
102 2011) or as endophytes in desert plants (Titus et al. 2002), due to mycorrhizae being
relatively sensitive to dry soil conditions (Aguilera et al. 2016). In contrast, the
104 majority of biocrust fungi are Ascomycota, with the Pleosporales being widespread
and dominant (Bates et al. 2012, Porrás-Alfaro et al. 2011). Pleosporales, along with
106 other Ascomycota fungal orders, contain dark septate endophytes (Jumpponen and
Trappe 1998). Dark septate endophytes are thermal- and drought-tolerant fungi due to
108 melanin-rich cell walls conferring protection from UV and drought stress (Gostincar
et al. 2010). Taken together, the prevalence of dark septate fungi in desert systems,
110 along with their ability to maintain metabolic activity under low water potentials
(Barrow 2003), makes these endophytes excellent candidates to translocate resources
112 in loops (Green et al. 2008).

114 Minor rainfall events may allow fungi to act as conduits and reservoirs for N. To
investigate the potential for biocrust constituents and N form to influence the
116 movement of N through the putative fungal loops, we created minor, localized rainfall
events and measured $\delta^{15}\text{N}$, from $^{15}\text{N-NH}_4^+$ and $^{15}\text{N-NO}_3^-$, within the surrounding dry
118 cyanobacteria- and moss-dominated crusts, and grass, *Achnatherum hymenoides*
(Indian ricegrass). In tandem with ^{15}N analyses, we estimated the biomass of two
120 major division of fungi (Ascomycota and Basidiomycota) and bacteria, and
characterized fungal communities by sequencing the 18S rRNA gene to identify
122 potential links between fungal taxa and ^{15}N movement.

124 **2 Materials and methods**

2.1 Site description

126 We conducted our study in two cold desert ecosystems of the Colorado Plateau, UT.
One site was near Castle Valley (40°05'27.43"N-112°18'18.24"W) and the other was
128 adjacent to the US Geological Survey (USGS) Southwest Biological Science Center
Research Station in Moab, UT (40°05'27.43"N-112°18'18.24"W). Rugose crusts
130 consisting of 22% moss *Syntrichia caninervis*, 5-7% cyano-lichens *Collema tenax*
and *Collema coccophorum* and 55% cyanobacteria cover the Castle Valley site
132 (Darrouzet-Nardi et al. 2015), while smooth, light algal crusts dominated by one
cyanobacterium, *Microcoleus vaginatus*, cover the USGS site. Across both sites,
134 vegetation is dominated by perennial grass *Achnatherum hymenoides* (Roem &
Schult) and the native perennial shrub *Atriplex confertifolia* (Torr. & Frém). Mean

136 annual temperature and precipitation at Castle Valley is 13°C and 269 mm, while the
USGS site is slightly warmer (MAT=13.8°C) and drier (MAP=189 mm; based on
138 1981-2010 data; WRCC 2017). Both soils are Aridisols with Castle Valley classified
as a sandy loam, calcareous Rizno series (Darrouzet-Nardi et al. 2015) and USGS as a
140 Bluechief series sandy loam.

142 **2.2 Simulated rainfall events and ¹⁵N form applications**

We simulated minor, localized rainfall events and measured $\delta^{15}\text{N}$, from $^{15}\text{N-NH}_4^+$ and
144 $^{15}\text{N-NO}_3^-$ rainfall events containing two isotopically-labeled, inorganic N forms and
tracked the movement of the label through our moss-dominated (Castle Valley) and
146 cyanobacteria-dominated biocrusts (USGS Station), and *A. hymenoides*. First, we
randomly selected six circular plots per site with a radius of 1.0 m and at least 10 m
148 apart from each other. Three plots were assigned to be labeled with K^{15}NO_3 (99 at.%)
and the other three plots to be labeled with $(^{15}\text{NH}_4)_2\text{SO}_4$ (99 at.%). Second, we
150 randomly selected five biocrust patches and five *A. hymenoides* along eight axes (e.g.,
N, NE, E, SE, S, SW, W, and NW) radiating from the center of each circular plot and
152 measured the radial distance to biocrusts or grasses. Third, we simulated a 2.5 mm
rainfall event by spraying 3 mL of deionized water solution and either isotopic label
154 (0.30 mg ^{15}N) onto a 5 cm diameter circle in the center of the circular plots (2 biocrust
types \times 3 circular plots locations \times 2 N forms \times \approx 10 samples [4 – 5 biocrusts or 4 – 7
156 *A. hymenoides* depending on grass density in the circular plot] = 137). For the isotopic
applications, either 2.60 g of 99 at.% K^{15}NO_3 or 1.70 g of 99 at.% $(^{15}\text{NH}_4)_2\text{SO}_4$ was

158 dissolved in 18 mL of deionized water to create a 1.43 M or 0.72 M solution,
respectively. The ^{15}N additions wetted the sandy loams (bulk density $\approx 1.5 \text{ g cm}^{-3}$) to
160 a depth of 1 cm and added approximately equal NH_4^+ ($10 \mu\text{g N g soil}^{-1}$) and double
 NO_3^- concentrations to surface soils (Sperry et al. 2006). All additions were
162 completed midday in April, as *A. hymenoides* were starting to set seed.

164 **2.3 Sample collection and ^{15}N analyses**

Biocrust and foliage samples were collected twenty-four hours after the simulated
166 rainfall event containing our different inorganic ^{15}N forms. Biocrusts were removed
as three subsamples from each biocrust location with a soil corer (2 cm diameter \times 5
168 cm length) to a depth of 2 mm. Crust distances away from the tracer application
ranged from 22 – 97 cm. The composited soil samples were kept cold (5°C) in the
170 field, split in the lab, and a portion of the soil was frozen (-20°C) until we performed
fungal and bacterial DNA analyses. We randomly selected five leaves from
172 *Achnatherum*, which ranged in distance anywhere from 29 – 120 cm away from the
tracer application and in volume from $0.002 - 0.048 \text{ m}^3$. The leaves and remaining
174 soils (sieved 2 mm) were air-dried, ground in a reciprocating tissue homogenizer, and
analyzed for ^{15}N using a PDZ Europa ANCA-GSL elemental analyzer, interfaced
176 with a PDZ Europa 20–20 isotope ratio mass spectrometer (Sercon Ltd., Cheshire,
UK) at the University of California Davis Stable Isotope Facility
178 (<http://stableisotopefacility.ucdavis.edu>). We expressed the resulting isotope ratios in
 δ notation as parts per thousand (‰) where:

180
$$\delta^{15}\text{N} = (R_{\text{sample}} / R_{\text{standard}}) \times 1000 \quad (1)$$

182 R is the molar ratio of the heavier to the lighter isotope ($^{15}\text{N}/^{14}\text{N}$) for the standard or
sample. To track the movement of inorganic N forms through our two biocrust types
(moss-lichen-dominated and cyanobacteria dominated biocrust) and into grasses, we
184 analyzed the relationships between $\delta^{15}\text{N}$ present in crust and leaf tissue to the distance
of the crust and *Achnatherum* by site by creating linear mixed effects models for the
186 biocrust type and N form combinations. In all models, distances of biocrusts or
grasses was nested within individual circular plots, and the three plots were treated as
188 a random factor to control for the impact of plot differences on our response variable.
All models were created with the *lm* function in R (R Development Core Team 2017).

190

2.4 Biomass estimations of major fungal components

192 To investigate the potential for fungi to translocate our ^{15}N forms, we estimated the
biomass of two major divisions of fungi (Ascomycota and Basidiomycota) and
194 bacteria in biocrusts using quantitative PCR. From the frozen biocrust samples, we
extracted genomic DNA using a DNeasy PowerLyzer PowerSoil Kit (Qiagen, MD,
196 USA) and quantified the gene copy numbers of Ascomycota and Basidiomycota on a
Mastercycler EP Realplex qPCR (Eppendorf, Hamburg, Germany) with SYBR Green.
198 We amplified division-specific regions of the internal transcribed spacer (ITS) with
primer pair ITS5 (forward) and ITS4A (reverse) for Ascomycota (Larena et al. 1999)
200 and ITS4B (forward) and 5.8sr (reverse) for Basidiomycota (Fierer et al. 2005). We
selected the universal bacterial 16S rRNA primer set EUB338, forward, and Eub518,

202 reverse, to estimate the biomass of bacteria (Aanderud et al. 2013). In 12.5 μ l
reactions, using KAPA2G Robust PCR Kits (KAPA Biosystems, Wilmington, MA,
204 USA), we amplified targeted genes using the following thermocycler condition: an
initial denaturation step at 94°C for 3 min followed by 35 cycles of denaturation at
206 94°C for 45 s, annealing at either at 55 °C (Ascomycota), 64°C (Basidiomycota), or
60°C (bacteria) for 30 s, and extension at 72°C for 90 sec. We generated qPCR
208 standards for Basidiomycota, Ascomycota, and bacteria from biocrusts using the
TOPO TA Cloning® Kit (ThermoFisher Scientific, MA, USA) as outlined by
210 Aanderud et al. (2013). The coefficients of determination (R^2) for our assays ranged
from 0.90 to 0.99, and amplification efficiencies fell between 0.99 and 1.92. We
212 analyzed the relationships between biocrust $\delta^{15}\text{N}$ and the gene copy number of
Ascomycota, Basidiomycota, and bacteria by creating linear mixed effects models for
214 each biocrust type and N form combination (2 biocrust types \times 3 circular plots
locations \times 2 N forms \times \approx 1 – 5 biocrusts = 48). DNA from eight moss-dominated and
216 four cyano-dominated biocrusts were difficult to amplify, especially one moss
biocrust circular plot reducing the number of replicants from five to one. We used the
218 *lm* function in R and treated plot as a random factor and gene copy number nested
within plot. We further tested for differences in our biomass estimates between the
220 crust types using multiple t-tests and a Benjamini-Hochberg correction to control for
the false discovery rate associated with multiple comparisons (Benjamini and
222 Hochberg 1995).

224 **2.5 Biocrust fungal communities**

To identify the fungal taxa participating in N translocation, we characterized fungal
226 communities in biocrusts using bar-coded sequencing. We PCR amplified the V9
region of the 18S rRNA gene using a universal eukaryote primer set, 1391F and
228 EukBr, with a unique 12-bp Golay barcode fused to EukBr (Amaral-Zettler et al.
2009, Hamady et al. 2008). Thermocycler parameters were similar to qPCR analyses
230 and consisted of a denaturation step at 94°C for 3 min, followed by 35 cycles of
denaturation at 94°C for 45 s, an annealing step at 57°C for 60 s, elongation at 72°C
232 for 90 s, and a final extension at 72°C for 10 min. We then purified and pooled PCR
amplicon libraries to near equimolar concentrations using SequalPrep™
234 Normalization Plate Kits (Invitrogen, Carlsbad, CA, USA) and quantified the
amplicon libraries by real-time qPCR using a KAPA Library Quantification Kit (Kapa
236 Biosystems, Wilmington, MA, USA). All samples were sequenced at the Brigham
Young University DNA Sequencing Center (<http://dnasc.byu.edu/>) using the Illumina
238 HiSeq 2500 platform (Illumina Biotechnology, San Diego, CA, USA), generating 2 ×
250 paired-end reads. Illumina sequence reads were analyzed within QIIME (v.
240 1.9.1), an open-source software pipeline suitable for microbial community analysis
(Caporaso et al. 2010). We removed barcodes and primers with a custom, in-house
242 script previous to joining paired-end reads by using fastq-join under default
parameters (Aronesty 2011). Joined reads were then de-multiplexed and checked for
244 chimeras (Haas et al. 2011). We then clustered the de-multiplexed reads into OTUs,
applying a similarity threshold of 97%, using QIIME's default OTU clustering tool-

246 uclust (Edgar et al. 2011). Taxonomies of representative OTUs were assigned using
uclust and the 18S rRNA gene SILVA 128 database which was clustered into OTUs
248 at 97% similarity (Quast et al. 2013). To evaluate if biocrust type supported similar
fungal composition, we calculated the relative recovery of 27 fungal orders, including
250 dark septate lineages. We tested for differences between biocrust types using t-tests
and a Benjamini-Hochberg correction (2 biocrust types \times 6 randomly selected
252 biocrusts = 12).

254 **3 Results**

3.1 Translocation of $^{15}\text{NH}_4^+$ in cyanobacteria biocrusts

256 The movement of ^{15}N was clearly apparent in cyanobacteria-dominated biocrusts
following the addition of $^{15}\text{NH}_4^+$, with $\delta^{15}\text{N}$ decreasing as the radial distance from the
258 central application point of $^{15}\text{NH}_4^+$ increased. In the overall model:

$$260 \quad \delta^{15}\text{N biocrust} = 51 - 0.71 (\text{distance}) + 0.06 (\text{distance} \times \text{plot}) \quad (\text{eq. 1})$$

262 ($R^2 = 0.67$, $F_{2,12} = 11$, $P = 0.002$, figure 1A), distance was significant ($P = 0.003$) and
possessed a negative slope. Surrounding the tracer application, $\delta^{15}\text{N}$ was enriched
264 upwards of 40‰ more than 20 cm away and continued to be enriched to
approximately 10‰ almost 100 cm away with enrichment ranging from 9.1 – 49‰.

266 There was no such relationship between $\delta^{15}\text{N}$ and the radial distance from any other
crust type or N form as demonstrated by the mixed effect models (cyanobacteria

268 biocrust $^{15}\text{NO}_3^-$ addition: $R^2 = 0.17$, $F_{2,12} = 1.2$, $P = 0.32$, figure 1B; moss biocrust
 $^{15}\text{NH}_4^+$ addition: $R^2 = 0.01$, $F_{2,12} = 0.07$, $P = 0.94$, figure 1A; and moss biocrust
270 $^{15}\text{NO}_3^-$ addition: $R^2 = 0.16$, $F_{2,12} = 1.2$, $P = 0.33$, figure 1B). The location of the three
circular plots was not a significant factor in any linear mixed effects models for
272 biocrusts.

274 3.2 Potential movement of $^{15}\text{NH}_4^+$ into grass leaves in cyanobacteria biocrusts

None of the label appeared to reach *A. hymenoides* leaves in either of the two types of
276 biocrusts. However, in cyanobacteria-dominated biocrusts where ^{15}N from $^{15}\text{NH}_4^+$
was translocated, the mixed effects model relating $\delta^{15}\text{N}$ from $^{15}\text{NH}_4^+$ into *A.*
278 *hymenoides* leaves was significant ($R^2 = 0.37$, $F_{2,17} = 5.1$, $P = 0.02$):

$$280 \delta^{15}\text{N leaves} = 3.1 - 0.03 (\text{distance}) + 0.01 (\text{distance} \times \text{plot}) \quad (\text{eq. 2})$$

282 and the radial distance was marginally significant ($P = 0.08$, data not shown). The
 $\delta^{15}\text{N}$ in leaves declined the further away the grass was from the ^{15}N application point,
284 with leaf enrichment between 1.0 – 6.7‰. In the other three models, the R^2 , F values,
and P -values of all other mixed effects models ranged from 0.06 – 0.10, 0.46 – 0.67,
286 and 0.54 – 0.64 respectively (data not shown). The $\delta^{15}\text{N}$ found in *A. hymenoides*
leaves was $2.6\text{‰} \pm 0.45$ (means \pm SEM) in cyanobacteria biocrusts exposed to $^{15}\text{NO}_3^-$
288 and $0.85\text{‰} \pm 0.47$ in moss biocrusts.

290 **3.3 $^{15}\text{NH}_4^+$ movement in cyanobacteria biocrusts related to Ascomycota**

The biocrust that translocated N also exhibited a robust relationship between the
292 proxy for Ascomycota biomass and biocrust $\delta^{15}\text{N}$. In cyanobacteria biocrusts, the
greater the gene copy number of Ascomycota the lower the $\delta^{15}\text{N}$ from $^{15}\text{NH}_4^+$. In the
294 overall model:

296
$$\delta^{15}\text{N} = 280 - 37 (\text{gene copy number Ascomycota}) + 1.1 (\text{distance} \times \text{plot}) \quad (\text{eq. 3})$$

298 ($R^2 = 0.63$, $F_{2,8} = 6.8$, $P = 0.02$, figure 2A), the proxy for Ascomycota biomass was
significant ($P = 0.01$) and negatively related to $\delta^{15}\text{N}$. In cyanobacteria crusts exposed
300 to $^{15}\text{NO}_3^-$, and in the moss-dominated crusts, however, there was no such relationship
between $\delta^{15}\text{N}$ from $^{15}\text{NO}_3^-$ and Ascomycota gene copy number (cyanobacteria crust
302 model: $R^2 = 0.08$, $F_{2,12} = 0.6$, $P = 0.58$, figure 2B; moss crust model: $R^2 = 0.16$, $F_{2,12} =$
1.2, $P = 0.33$, figure 2B) or in moss crusts exposed to $^{15}\text{NH}_4^+$ additions ($R^2 = 0.01$,
304 $F_{2,12} = 0.07$, $P = 0.94$, figure 2A). Basidiomycota and bacteria biomass in both crust
types was not related to either N form (data not shown). The biomass estimates of all
306 measured biocrust components were consistently higher in moss- than cyanobacteria-
dominated crusts. Basidiomycota biomass was $1.5 \times 10^9 \pm 5.5 \times 10^8$ in cyanobacteria and
308 $5.8 \times 10^9 \pm 7.2 \times 10^8$ in moss biocrusts (t-test, $t = 4.5$, $P < 0.0001$, $df = 1$, data not
shown). Ascomycota biomass was $2.6 \times 10^7 \pm 4.5 \times 10^6$ in cyanobacteria and 1.1×10^8
310 $\pm 2.4 \times 10^7$ in moss biocrusts (t-test, $t = 3.3$, $P = 0.003$, $df = 1$). Bacterial biomass was at
least two orders of magnitude lower in cyanobacteria biocrusts

312 (cyanobacteria= $5.5 \times 10^6 \pm 8.9 \times 10^5$ and moss crusts= $2.7 \times 10^7 \pm 4.8 \times 10^6$, (t-test, $t = 4.5$,
314 $P < 0.0001$, $df = 1$).

3.4 Dark septate fungi as major components of biocrusts

316 Four of the nine fungal orders, known to contain dark septate endophyte members,
were present in both biocrust types, with the Pleosporales and Pezizales being
318 dominant taxa. In biocrusts, fungi comprised much of eukaryotic community
(cyanobacteria = $30\% \pm 4.7$ and moss = $33\% \pm 4.0$), Ascomycota was the most
320 common fungal division (cyanobacteria = $82\% \pm 2.8$ and moss = $87\% \pm 2.9$), and
orders with known dark septate members accounted for at least 67% of the
322 Ascomycota (cyanobacteria = $83\% \pm 4.8$ and moss = $67\% \pm 8.6$, figure 3). In
cyanobacteria biocrusts, Pleosporales accounted for 66% (± 6.9) of all dark septates
324 and the recovery of this taxa was twice as high in cyanobacteria- than moss-
dominated crusts (t-test, $t = 03.0$, $P = 0.01$, $df = 1$). Even though the relative
326 abundance of Pleosporales differed, the number of gene copies of Pleosporales was
similar between the two biocrusts (cyanobacteria = $1.7 \times 10^7 \pm 6.3 \times 10^6$ and
328 moss= $2.9 \times 10^7 \pm 1.3 \times 10^7$, t-test, $t = 0.99$, $P = 0.35$, $df = 1$) as determined by an
extrapolation of qPCR values in conjunction with percent recovery of taxa for
330 Ascomycota. The *Pezizales* comprised a relatively large percentage of the biocrust
community in moss-dominated biocrust with a recovery of 15% (± 8.3) and 28% (\pm
332 9.0) in cyanobacteria- and moss-dominated crusts, respectively (t-test, $t = 1.1$, $P =$

0.32, $df = 1$). Eukaryotic community data was based on the recovery of 1,232,312

334 quality sequences and 5,176 unique OTUs.

336 **4 Discussion**

In biological networks, the magnitude and direction of resource transfer in fungi is
338 predominantly thought to be influenced by the physiological source-sink gradients
created by individual plants (Fellbaum et al. 2014) or between plants (Weremijewicz
340 et al. 2016). However, fungi may be more than just passive conduits by exerting
control over resources due to their own sink-source resource needs (Simard and
342 Durall 2004). Our findings suggest that a minor, localized rainfall event may initiate
fungal loops by allowing the rapid translocation of N in biocrusts at a rate of 40 mm
344 h^{-1} in twenty-four hours. The movement of N was only apparent in the cyanobacteria-
dominated crusts, where $\delta^{15}\text{N}$ decreased as the distance from the addition of the
346 $^{15}\text{NH}_4^+$ label increased. Further, the presence of Ascomycota was related to the
amount of biocrust $\delta^{15}\text{N}$ from $^{15}\text{NH}_4^+$, with the isotope being diluted in soils with
348 higher levels of Ascomycota biomass. Eighty-three percent of the Ascomycota were
from four fungal orders containing known dark septate endophytes and 66% of these
350 taxa were from one order, the Pleosporales. Taken together, our results suggest that
fungal loops are potentially structured by fungal constituents, especially Pleosporales,
352 translocating N from NH_4^+ over NO_3^- .

354 **4.1 Fungal loops only in cyanobacteria-dominated crusts**

Our findings suggest that fungal loops do occur in cyanobacteria-dominated biocrusts.

356 Biocrust components, predominantly cyanobacteria, are known to fix and secrete up
to 50% of their newly fixed C and 88% of N into surrounding soils within minutes to
358 days of fixation, depending on precipitation characteristics (Belnap et al. 2003). Thus,
active crust constituents may exude resources for other biocrust constituents, such as
360 fungi, to acquire and initiate fungal loops. Our results are similar to Green et al.
(2008) whose previous work identified loops in cyanobacteria biocrusts moving ^{15}N
362 from isotopically labeled nitrate in the Chihuahuan Desert. Although we only found
movement of ^{15}N as labeled ammonium, our label moved at a comparable rate to
364 Green et al. (2008; 40 mm h⁻¹ versus 44 mm h⁻¹, respectively). The lack of ^{15}N
movement from labeled nitrate in our study may stem from the short time period that
366 we employed to measure translocation. When Green et al. (2008) evaluated ^{15}N
movement at two time points, 24 hours and four days after tracer application, they
368 found that biocrust enrichment consistently increased over time. Therefore, if we had
continued to assess biocrusts isotopic signatures after 24 hours, we potentially could
370 have captured the movement of labeled nitrate as well.

372 **4.2 Addressing the lack of loops in moss-dominated crusts**

The seeming lack of loops in moss-dominated crusts may stem from the relatively
374 large moss biomass of *S. caninervis* effectively absorbing and holding N from our
minor wet deposition event. We measured elevated levels of biomass of all biocrust
376 constituents (i.e., mosses, fungi, and bacteria) in moss-dominated relative to

378 cyanobacteria-dominated biocrusts. If most biocrust constituents were N limited,
including mosses, then the ^{15}N was possibly retained in place to meet N deficiencies
before being disseminated to other crust constituents outside the application zone. The
380 ability of mosses to scavenge atmospheric deposited N is well recognized in other
systems (Liu et al. 2013, Fritz et al. 2014). Most mosses acquire N from either
382 wet/dry atmospheric deposition (Yaunming et al. 2016) or as biogenic sources from
cyanobacterial associations on their leaves (Rousk et al. 2013). Mosses do alter N
384 dynamics in arid environments. When *S. caninervis* was lost from our system, a
dramatic increase in nitrification rates were observed (Reed et al. 2012). The higher
386 levels of nitrification were most likely supported by the decomposition of dead moss
biomass and subsequent release of new NH_4^+ ; however, after the moss mortality,
388 inorganic N pooled as NO_3^- , in the remaining cyanobacteria-dominated biocrust.
Thus, the presence or absence of mosses has the potential to alter N pools and fluxes
390 in biocrusts.

The lack of ^{15}N movement in moss-dominated crusts may reside in the nature of
392 our minor rainfall event. Our moss, *S. caninervis*, became photosynthetically active
following the 2 mm rainfall event, changing in color from brown to green, but only in
394 the discrete biocrust patches that we watered. Mosses, including *S. caninervis*, are
stimulated by minor rainfall events (Wu et al. 2014), with events as small as 1 mm
396 activating moss photosynthesis (Coe et al. 2012). Our rainfall event was intended to
wet a small circle of biocrust to a depth of 1 cm. However, the additional
398 aboveground biomass of mosses and the rugose topography of moss-dominated crusts

relative to the smooth cyanobacteria-dominated crusts may have limited the depth our
400 minor rainfall event penetrated the soil and, in turn, activated other biocrust
components. Also, water from our event might have evaporated more quickly from
402 the mossy biocrust surface, limiting the activity time of all constituents involved. To
more conclusively determine the potential for fungal loops to exist in moss-dominated
404 biocrusts, more information is needed to determine the importance of effective
rainfall size in initiating fungal loops.

406 N may move differently in moss-dominated biocrusts compared to other biocrust
types. If desert mosses have fungal associations, then fungi have the potential to move
408 sequestered N to the mosses in a new kind of loop. Rhizoids and thalli of bryophytes
may contain fungal associations (Pressel et al. 2010). Dark septate endophytes
410 colonize mosses (Day and Currah 2011). Taken together, the exchange of
photosynthate and N may occur in a tighter, more localized loop between mosses and
412 dark septate fungi, even following a minor rainfall event.

414 **4.3 Loops may preferentially move NH_4^+ over NO_3^-**

We found that NH_4^+ , but not NO_3^- , was rapidly translocated within cyanobacterial
416 crusts. The enrichment of $\delta^{15}\text{N}$ from $^{15}\text{NH}_4^+$ in cyanobacteria biocrusts was related to
our proxy for Ascomycota biomass and potentially dark septate fungi due to their
418 dominance in our sequencing effort. We explain the negative relationship between
Ascomycota gene copy number and $\delta^{15}\text{N}$ signal as a simple dilution—the higher our
420 biomass estimates of Ascomycota, the more spread in the ^{15}N signal. Although the

physiology of dark septate fungi remains relatively unexplored, if our desert fungi are
422 like most other fungi, then the preferential movement of NH_4^+ is understandable.
Generally, fungi prefer NH_4^+ over NO_3^- (Eltrop and Marschner 1996), as NH_4^+ is
424 readily acquired by fungi and assimilated into amino acids. After NH_4^+ uptake and
assimilation via the glutamate synthase or GS/GOGAT cycle, N is incorporated into
426 arginine through the urea cycle (Jin et al. 2012) due to the direct assimilation of NH_4^+
into the GS/GOGAT pathway (Courtly et al., 2015). Thus, NH_4^+ is most likely
428 transformed into arginine and moved within mycelium by amino acid transporters
(Govindarajulu et al. 2005, Garcia et al. 2016). There is some evidence for the
430 importance of amino acid transporters in fungal endophytes, as arbuscular
colonization leads to an increase in the uptake of arginine and multiple other amino
432 acids (e.g., phenylalanine, lysine, asparagine, histidine, methionine, tryptophan, and
cysteine) by their host plants (Whiteside et al. 2012). However, to verify the
434 movement of N through Ascomycota and the role of biomass in translocation, a more
direct approach is needed. For example, quantum dots (fluorescent nanoscale
436 semiconductors) have tracked the flow of organically derived N into arbuscular
mycorrhizae and into *Poa annua* in less than 24 hours (Whiteside et al. 2009). The N
438 form NO_3^- did move into our cyanobacteria crusts but not nearly to the extent reported
by Green et al. (2008). Besides fungal preferences, other factors may play a role in the
440 uptake of N, such as the increase in mobility of NO_3^- in soils, differences in soil
cation exchange capacity due to clay content, or fungi capitalizing on the more
442 abundant N form specific to a soil. Unfortunately, based on our design, we were

unable to distinguish the form of N captured or translocated by biocrust constituents.

444 More information is needed to identify the importance of N form and the movement
of organic N within fungal loops.

446

4.4 Dark septate and Pleosporales as conduits

448 Our results support the idea that Pleosporales are the most likely conduits for N. Four
of the nine fungal orders we identified contained known dark septate endophytes with
450 one order, Pleosporales, being the most abundant. The Pleosporales accounted for
66% of the Ascomycota taxa in cyanobacteria crusts. Based on the relationship
452 between $\delta^{15}\text{N}$ and Ascomycota biomass, the overwhelming abundance of
Pleosporales, and the universal occurrence of Ascomycota in biocrusts, the
454 Pleosporales assumedly play a role in fungal loops. We are not the first to reach this
conclusion. Green et al. (2008) also identified Pleosporales as being the primary
456 candidate involved in fungal loops. In their semi-arid grassland, Pleosporales were the
most common taxa on *Bouteloua* roots, in the rhizosphere, and in biocrusts. We found
458 799 operational taxonomic units, based on 97% similarity, with all of the identifiable
sequences, belonging to three genera: *Leptosphaeria* (1.6% of Pleosporales
460 sequences), *Morosphaeria* (3.8% of Pleosporales sequences), and *Ophiosphaerella*
(8.1% of Pleosporales sequences; data not shown). *Leptosphaeria* and
462 *Ophiosphaerella* may be pathogenic endophytes on grass species (Martin et al. 2001,
Yuan et al. 2017), but may also be beneficial by delaying and reducing the symptoms
464 of other fungal pathogens (Yuan et al. 2017). However, 86% of our Pleosporales taxa

were unidentifiable based on our target genetic region and are potentially novel,
466 suggesting that much remains unknown about dark septates in deserts. Further
research is needed to address the theory of Pleosporales conduits in biocrusts and the
468 ecological importance of the dark septate endophytes in desert systems.

470 **4.5 Little N translocation to grass**

Due to the discrete nature of our minor, localized rainfall event, we were not surprised
472 that little of the label entered the leaves of *A. hymenoides*. In the fungal loop
hypothesis, a larger rainfall event triggers the plant to become a sink for the N
474 building up in fungi over previous minor rainfall events. We conducted our
experiment absent of a larger rainfall event and our 2.5 mm rainfall event was applied
476 over a 5 cm diameter circle of soil in early summer. When a similar precipitation
event size (2 mm) was applied across a much larger area (4 x 4 m² plot) on Colorado
478 Plateau soils during spring or summer, the predawn water potential of *A. hymenoides*
was similar one day after and one day prior to watering (Schwinning et al. 2003).
480 Thus, our minor rainfall event most likely failed to alter the water status of the grass
or cause grasses to become a sink for N. However, we did find some evidence of ¹⁵N
482 in *A. hymenoides* leaves following our ¹⁵NH₄⁺ application in cyanobacteria-dominated
crusts. The pattern of the enrichment, a dilution with increasing distance from the
484 application point, was similar to the pattern found in biocrusts, but the most enriched
leaves (6.7‰) were less than the least enriched crust (9.1‰). Even though the
486 enrichment was minor, the presence of ¹⁵N in *A. hymenoides* provides some evidence

of biocrust constituents being linked to plants and the translocation of N occurring
488 even in the absence of a larger rainfall event to enhance grass activity. In April, at the
time of the experiment, *A. hymenoides* was photosynthetically active. If we had added
490 more label or evaluated the isotope signature of roots, we may have detected more ¹⁵N
label in grass tissue.

492

5. Conclusion

494 Cyanobacterial biocrusts are potentially interconnected in extensive biological
networks. In light of the absence of N movement in moss-dominated crusts, mosses
496 may hinder fungal loops. The abundant moss biomass in some biocrust may absorb
and retain the applied N label. Due to the dominance of dark septate endophytes in
498 biocrusts, fungi may act as conduits within the network. Our results add to the indirect
evidence of fungal loops, but more information is needed to quantify the
500 environmental conditions and biocrust constituents controlling the magnitude and
directionality of the translocation of N to vascular plants.

502

Acknowledgements The portion of the research conducted by Dr. Wu and Dr.

504 Yuanming was funded by National Natural Science Foundation of China (grant #
41571256 and 41771299). Dr. Belnap thanks the Ecosystems Program of U.S.
506 Geological Survey. Any use of trade, firm, or product names is for descriptive
purposes only and does not imply endorsement by the U.S. Government.

508

Author contributions ZTA and JB designed the study. ZTA, TBS, NW, AST, and JB
510 conducted the experiments. ZTA, TBS, NW, AST, YZ, and JB analyzed and
interpreted the data. ZTA, TBS, NW, AST, YZ, and JB helped write and review the
512 manuscript. ZTA agrees to be accountable for all aspects of the work in ensuring that
questions related to the accuracy or integrity of any part of the work are appropriately
514 investigated and resolved.

516 **Conflict of interest** The authors declare no conflict of interest.

518

520 **Figure legend**

Figure 1 Cyanobacteria biocrusts facilitated the translocation of N from $^{15}\text{NH}_4^+$ in twenty-four hours. Based on linear mixed effects models, $\delta^{15}\text{N}$, from $^{15}\text{NH}_4^+$, ($R^2 = 0.67$, $F_{2,12} = 11$, $P = 0.002$, A) decreased as the radial distance from the isotopic application increased. There was no such relationship between $\delta^{15}\text{N}$ and the radial distance from any other crust type or N form (A, B) Values are $\delta^{15}\text{N}$ (‰) from two biocrust types, cyanobacteria- and moss-dominated crusts, across circular plots (radius of 1.0 m) with a central application (5 cm diameter circle) of $^{15}\text{NH}_4^+$ or $^{15}\text{NO}_3^-$ in a simulated, minor rainfall event.

Figure 2 Ascomycota biomass influenced the distance N traveled. In cyanobacteria crusts, $\delta^{15}\text{N}$, from $^{15}\text{NH}_4^+$, was diluted as Ascomycota gene copy number increased ($R^2 = 0.63$, $F_{2,8} = 6.8$, $P = 0.02$, A). A similar pattern was not apparent in any other crust type or N form (A, B). Values are $\delta^{15}\text{N}$ (‰) from biocrusts and Ascomycota gene copy numbers, an approximation of biomass, from qPCR of the ITS region with primer pair ITS5 and ITS4A.

536

Figure 3 Pleosporales were the dominant Ascomycota order and contained dark septate species. Pie chart values are means ($n=6$) of the relative recovery from nine fungal orders, four of which contain dark septate endophytic taxa. Recovery was based on OTUs from eukaryotic community libraries of the 18S rRNA gene (97% similarity cutoff).

References cited

- 544 Aanderud ZT, Jones SE, Schoolmaster DR, Fierer N, Lennon JT. 2013. Sensitivity of
soil respiration and microbial communities to altered snowfall. *Soil Biology &*
546 *Biochemistry* 57:217-227.
- Aguilera LE, Armas C, Cea AP, Gutierrez JR, Meserve PL, Kelt DA. 2016. Rainfall,
548 microhabitat, and small mammals influence the abundance and distribution of soil
microorganisms in a Chilean semi-arid shrubland. *Journal of Arid Environments*
550 126:37-46.
- Amaral-Zettler LA, McCliment EA, Ducklow HW, Huse SM. 2009. A method for
552 studying protistan diversity using massively parallel sequencing of V9
hypervariable regions of small-subunit ribosomal RNA genes. *PLOS ONE* (art.
554 e6372)
- Aronesty E. 2011. Command-line tools for processing biological sequence data.
556 *Expression Analysis*. (14 October 2017;
<https://github.com/ExpressionAnalysis/ea-utils>)
- 558 Barrow JR. 2003. Atypical morphology of dark septate fungal root endophytes of
Bouteloua in arid southwestern USA rangelands. *Mycorrhiza* 13:239-247.
- 560 Bates ST, Nash TH, Garcia-Pichel F. 2012. Patterns of diversity for fungal
assemblages of biological soil crusts from the southwestern United States.
562 *Mycologia* 104:353-361.
- Behie SW, Bidochka MJ. 2014. Nutrient transfer in plant-fungal symbioses. *Trends in*
564 *Plant Science* 19:734-740.

- 566 Belnap J, Hawkes CV, Firestone MK. 2003. Boundaries in miniature: Two examples
from soil. *BioScience* 53:739-749.
- 568 Belnap J, Phillips SL, Sherrod SK, Moldenke A. 2005. Soil biota can change after
exotic plant invasion: does this affect ecosystem processes? *Ecology* 86:3007-
3017.
- 570 Benjamini Y, Hochberg Y. 1995. Controlling the false discovery rate: a practical and
powerful approach to multiple testing. *Journal of the Royal Statistical Society*
572 *Series B: (Methodological)* 57:289-300.
- 574 Cable JM, Huxman TE. 2004. Precipitation pulse size effects on Sonoran Desert soil
microbial crusts. *Oecologia* 141:317-324.
- 576 Caporaso JG, et al. 2010. QIIME allows analysis of high-throughput community
sequencing data. *Nature Methods* 7:335-336.
- 578 Coe KK, Belnap J, Sparks JP. 2012. Precipitation-driven carbon balance controls
survivorship of desert biocrust mosses. *Ecology* 93: 1626-1636
- 580 Collins SL, Sinsabaugh RL, Crenshaw C, Green L, Porras-Alfaro A, Stursova M,
Zeglin LH. 2008. Pulse dynamics and microbial processes in aridland ecosystems.
Journal of Ecology 96:413-420.
- 582 Collins SL, et al. 2014. A multiscale, hierarchical model of pulse dynamics in arid-
land ecosystems. *Annual Review of Ecology, Evolution, and Systematics* 45:397-
584 419.

Darrouzet-Nardi A, Reed SC, Grote EE, Belnap J. 2015. Observations of net soil
586 exchange of CO₂ in a dryland show experimental warming increases carbon losses
in biocrust soils. *Biogeochemistry* 126:363-378.

588 Day MJ, Currah RS. 2011. Role of selected dark septate endophyte species and other
hyphomycetes as saprobes on moss gametophytes. *Botany-Botanique* 89:349-359.

590 Edgar RC, Haas BJ, Clemente JC, Quince C, Knight R. 2011. UCHIME improves
sensitivity and speed of chimera detection. *Bioinformatics* 27:2194-2200.

592 Eltrop L, Marschner H. 1996. Growth and mineral nutrition of non-mycorrhizal and
mycorrhizal Norway spruce (*Picea abies*) seedlings grown in semi-hydroponic
594 sand culture. *New Phytologist* 133:469-478.

Fellbaum CR, Mensah JA, Cloos AJ, Strahan GE, Pfeffer PE, Kiers ET, Bucking H.
596 2014. Fungal nutrient allocation in common mycorrhizal networks is regulated by
the carbon source strength of individual host plants. *New Phytologist* 203:646-
598 656.

Fierer N, Jackson JA, Vilgalys R, Jackson RB. 2005. Assessment of soil microbial
600 community structure by use of taxon-specific quantitative PCR assays. *Applied
and Environmental Microbiology* 71:4117-4120.

602 Fritz C, Lamers LPM, Riaz M, van den Berg LJJ, Elzenga T. 2014. Sphagnum
mosses-masters of efficient N-uptake while avoiding intoxication. *PLOS ONE*
604 (art. e79991).

Garcia K, Doidy J, Zimmermann SD, Wipf D, Courty PE. 2016. Take a trip through
606 the plant and fungal transportome of mycorrhiza. *Trends in Plant Science* 21:937-
950.

608 Gostincar C, Grube M, de Hoog S, Zalar P, Gunde-Cimerman N. 2010.
Extremotolerance in fungi: evolution on the edge. *FEMS Microbiology Ecology*
610 71:2-11.

Govindarajulu M, Pfeffer PE, Jin HR, Abubaker J, Douds DD, Allen JW, Bucking H,
612 Lammers PJ, Shachar-Hill Y. 2005. Nitrogen transfer in the arbuscular
mycorrhizal symbiosis. *Nature* 435:819-823.

614 Green LE, Porras-Alfaro A, Sinsabaugh RL. 2008. Translocation of nitrogen and
carbon integrates biotic crust and grass production in desert grassland. *Journal of*
616 *Ecology* 96:1076-1085.

Haas BJ, et al. 2011. Chimeric 16S rRNA sequence formation and detection in Sanger
618 and 454-pyrosequenced PCR amplicons. *Genome Research* 21:494-504.

Hamady M, Walker JJ, Harris JK, Gold NJ, Knight R. 2008. Error-correcting
620 barcoded primers for pyrosequencing hundreds of samples in multiplex. *Nature*
Methods 5:235-237.

622 Hattenschwiler S, Tiunov AV, Scheu S. 2005. Biodiversity and litter decomposition
in terrestrial ecosystems. *Annual Review of Ecology* 36:191-218.

624 He XH, Critchley C, Bledsoe C. 2003. Nitrogen transfer within and between plants
through common mycorrhizal networks (CMNs). *Critical Reviews in Plant*
626 *Sciences* 22:531-567.

- Huxman TE, Snyder KA, Tissue D, Leffler AJ, Ogle K, Pockman WT, Sandquist DR,
628 Potts DL, Schwinning S. 2004. Precipitation pulses and carbon fluxes in semiarid
and arid ecosystems. *Oecologia* 141:254-268.
- 630 Jin HR, Liu J, Huang XW. 2012. Forms of nitrogen uptake, translocation, and transfer
via arbuscular mycorrhizal fungi: A review. *Science ChinaLife Sciences* 55:474-
632 482.
- Johnson NC, Graham JH, Smith FA. 1997. Functioning of mycorrhizal associations
634 along the mutualism-parasitism continuum. *New Phytologist* 135:575-586.
- Jumpponen A, Trappe JM. 1998. Dark septate endophytes: a review of facultative
636 biotrophic root-colonizing fungi. *New Phytologist* 140:295-310.
- Larena I, Salazar O, Gonzalez V, Julian MC, Rubio V. 1999. Design of a primer for
638 ribosomal DNA internal transcribed spacer with enhanced specificity for
ascomycetes. *Journal of Biotechnology* 75:187-194.
- 640 Liu XY, Koba K, Makabe A, Li XD, Yoh M, Liu CQ. 2013. Ammonium first: natural
mosses prefer atmospheric ammonium but vary utilization of dissolved organic
642 nitrogen depending on habitat and nitrogen deposition. *New Phytologist* 199:407-
419.
- 644 Martin DL, Bell GE, Baird JH, Taliaferro CM, Tisserat NA, Kuzmic RM, Dobson
DD, Anderson JA. 2001. Spring dead spot resistance and quality of seeded
646 bermudagrasses under different mowing heights. *Crop Science* 41:451-456.
- Osono T. 2007. Ecology of ligninolytic fungi associated with leaf litter
648 decomposition. *Ecological Research* 22:955-974.

650 Porras-Alfaro A, Herrera J, Natvig DO, Lipinski K, Sinsabaugh RL. 2011. Diversity
and distribution of soil fungal communities in a semiarid grassland. *Mycologia*
103:10-21.

652 Pressel S, Bidartondo MI, Ligrone R, Duckett JG. 2010. Fungal symbioses in
bryophytes: new insights in the twenty first century. *Phytotaxa* 9:238-253.

654 Quast C, Pruesse E, Yilmaz P, Gerken J, Schweer T, Yarza P, Peplies J, Glockner FO.
2013. The SILVA ribosomal RNA gene database project: improved data
656 processing and web-based tools. *Nucleic Acids Research* 41:D590-D596.

R Development Core Team, 2017. R: A language and environment for statistical
658 computing. R Foundation for Statistical Computing, Vienna, Austria, URL
<http://www.R-project.org>.

660 Reed SC, Coe KK, Sparks JP, Housman DC, Zelikova TJ, Belnap J. 2012. Changes to
dryland rainfall result in rapid moss mortality and altered soil fertility. *Nature*
662 *Climate Change* 2:752-755.

Rousk K, Jones DL, DeLuca TH. 2013. Moss-cyanobacteria associations as biogenic
664 sources of nitrogen in boreal forest ecosystems. *Frontiers in Microbiology* 4: 150.

Saikkonen K, Wali P, Helander M, Faeth SH. 2004. Evolution of endophyte-plant
666 symbioses. *Trends in Plant Science* 9:275-280.

Schneider T, Keiblinger KM, Schmid E, Sterflinger-Gleixner K, Ellersdorfer G,
668 Roschitzki B, Richter A, Eberl L, Zechmeister-Boltenstern S, Riedel K. 2012.
Who is who in litter decomposition? Metaproteomics reveals major microbial
670 players and their biogeochemical functions. *ISME Journal* 6:1749-1762.

Simard SW, Durall DM. 2004. Mycorrhizal networks: a review of their extent,
672 function, and importance. *Canadian Journal of Botany* 82:1140-1165.

Sperry LJ, Belnap J, Evans RD. 2006. *Bromus tectorum* invasion alters nitrogen
674 dynamics in an undisturbed arid grassland ecosystem. *Ecology* 87:603-615.

Schwinning S, Starr BL, Ehleringer JR. 2003. Dominant cold desert plants do not
676 partition warm season precipitation by event size. *Ecosystems Ecology* 136:252-
260.

678 Titus JH, Titus PJ, Nowak RS, Smith SD. 2002. Arbuscular mycorrhizae of Mojave
Desert plants. *Western North American Naturalist* 62:327-334.

680 van der Heijden MGA, Horton TR. 2009. Socialism in soil? The importance of
mycorrhizal fungal networks for facilitation in natural ecosystems. *Journal of*
682 *Ecology* 97:1139-1150.

Walder F, Niemann H, Natarajan M, Lehmann MF, Boller T, Wiemken A. 2012.
684 Mycorrhizal networks: common goods of plants shared under unequal terms of
trade. *Plant Physiology* 159:789-797.

686 Wang C, et al. 2014. Aridity threshold in controlling ecosystem nitrogen cycling in
arid and semi-arid grasslands. *Nature Communications* (art. 4799).

688 Welter JR, Fisher SG, Grimm NB. 2005. Nitrogen transport and retention in an arid
land watershed: Influence of storm characteristics on terrestrial-aquatic linkages.
690 *Biogeochemistry* 76:421-440.

Weremijewicz J, Sternberg L, Janos DP. 2016. Common mycorrhizal networks
692 amplify competition by preferential mineral nutrient allocation to large host
plants. *New Phytologist* 212:461-471.

694 Whiteside MD, Treseder KK, Atsatt PR. 2009. The brighter side of soils: quantum
dots track organic nitrogen through fungi and plants. *Ecology* 90:100-108.

696 Whiteside MD, Garcia MO, Treseder KK. 2012. Amino Acid Uptake in Arbuscular
Mycorrhizal Plants. *PLOS ONE* (art. e47643).

698 Wu N, Zhang YM, Downing A, Aanderud ZT, Tao Y, Williams S. 2014. Rapid
adjustment of leaf angle explains how the desert moss, *Syntrichia caninervis*,
700 copes with multiple resource limitations during rehydration. *Functional Plant
Biology* 41:168-177.

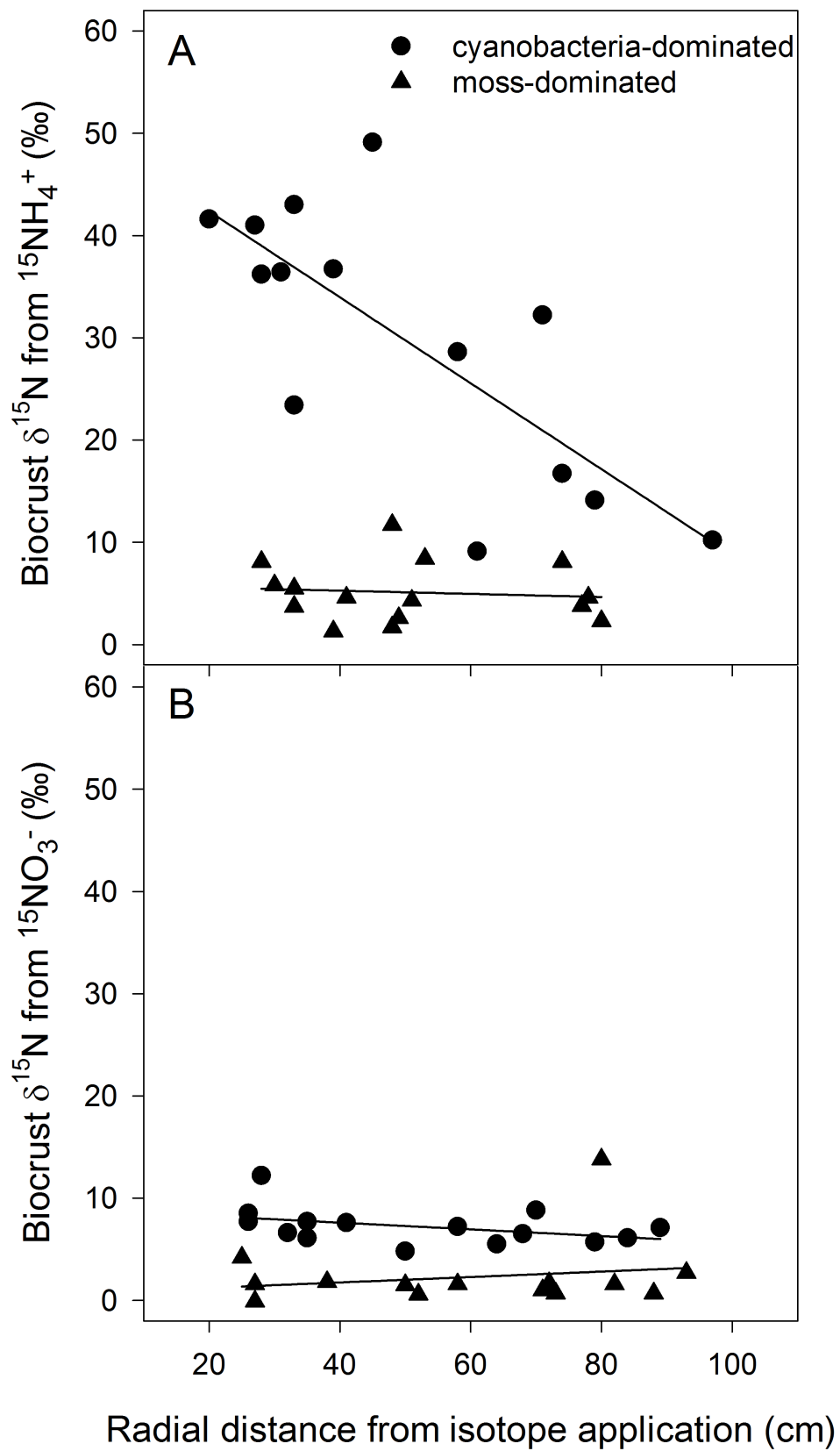
702 Yahdjian L, Sala OE. 2010. Size of precipitation pulses controls nitrogen
transformation and losses in an arid Patagonian ecosystem. *Ecosystems* 13:575-
704 585.

Yuan Y, Feng HJ, Wang LF, Li ZF, Shi YQ, Zhao LH, Feng ZL, Zhu HQ. 2017.
706 Potential of endophytic fungi isolated from cotton roots for biological control
against verticillium wilt disease. *PLOS ONE* (art. e0170557):12.

708 Zelikova TJ, Housman DC, Grote EE, Neher DA, Belnap J. 2012. Warming and
increased precipitation frequency on the Colorado Plateau: implications for
710 biological soil crusts and soil processes. *Plant and Soil* 355:265-282.

712

Figure 1



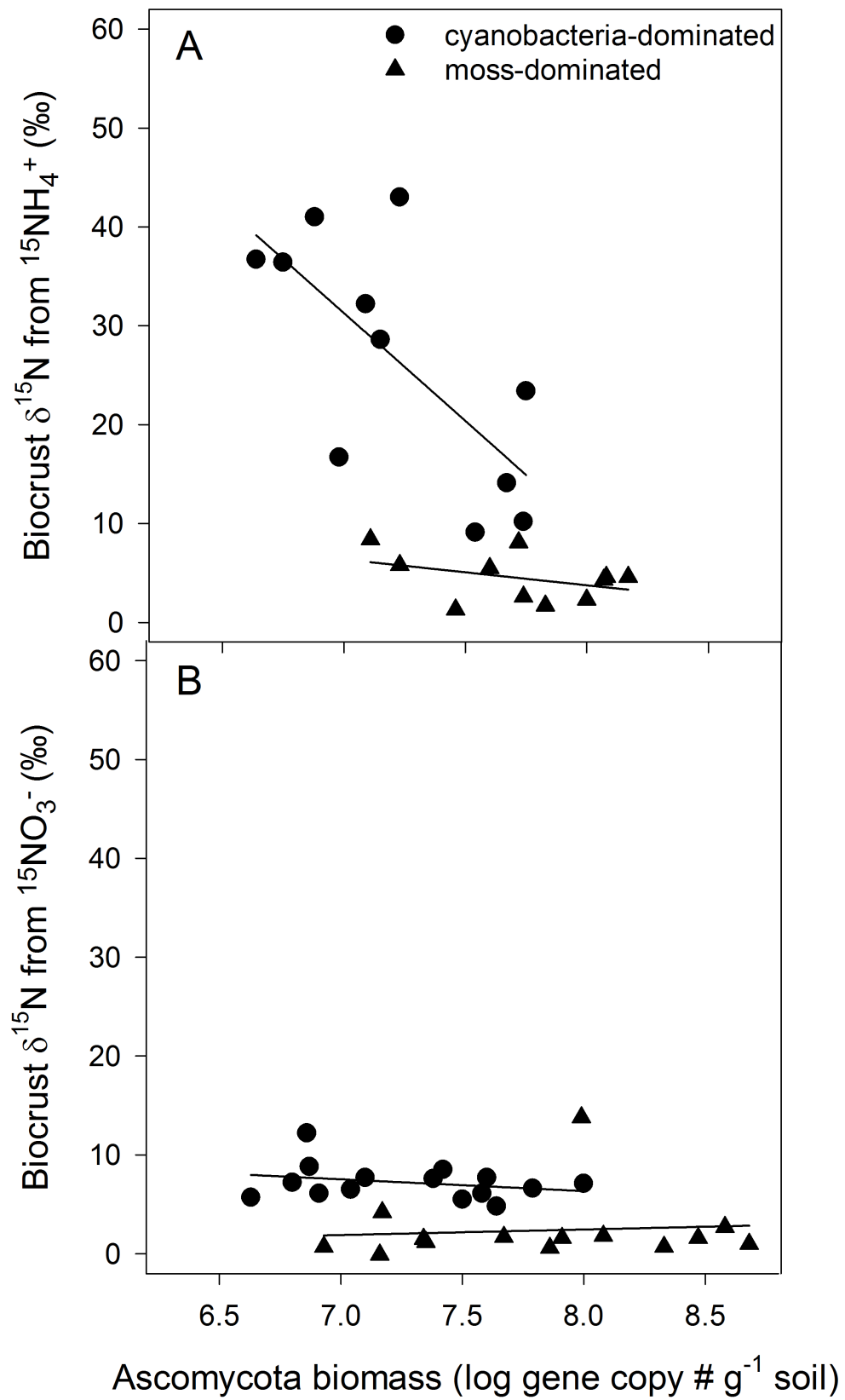
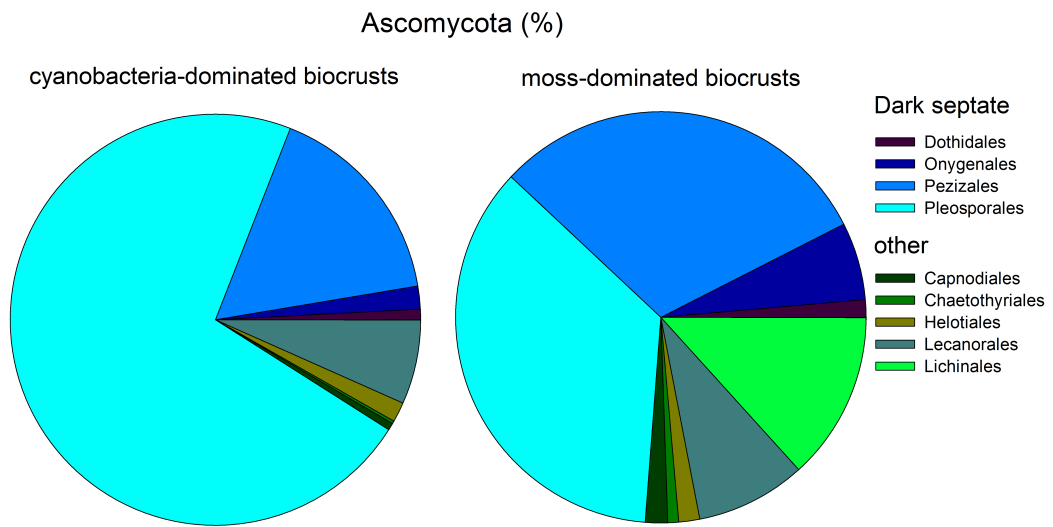


Figure 3



720

722